

Article

Using Regression Analysis for Automated Material Selection in Smart Manufacturing

Ivan Pavlenko ¹, Ján Piteľ ², Vitalii Ivanov ³, Kristina Berladir ⁴, Jana Mižáková ^{2,*}, Vitalii Kolos ³
and Justyna Trojanowska ⁵

¹ Department of Computational Mechanics Named after Volodymyr Martynovskyy, Sumy State University, 40007 Sumy, Ukraine; i.pavlenko@omdm.sumdu.edu.ua

² Department of Industrial Engineering and Informatics, Faculty of Manufacturing Technologies, Technical University of Košice, Bayerova 1, 080 01 Prešov, Slovakia; jan.pitel@tuke.sk

³ Department of Manufacturing Engineering, Machines and Tools, Sumy State University, 40007 Sumy, Ukraine; ivanov@tmvi.sumdu.edu.ua (V.I.); v.kolos@tmvi.sumdu.edu.ua (V.K.)

⁴ Department of Applied Materials Science and Technology of Constructional Materials, Sumy State University, 2, Rymskogo-Korsakova St., 40007 Sumy, Ukraine; kr.berladir@pmtkm.sumdu.edu.ua

⁵ Department of Production Engineering, Poznan University of Technology, 5, M. Skłodowskiej-Curie Sq., 60-965 Poznan, Poland; justyna.trojanowska@put.poznan.pl

* Correspondence: jana.mizakova@tuke.sk

Abstract: In intelligent manufacturing, the phase content and physical and mechanical properties of construction materials can vary due to different suppliers of blanks manufacturers. Therefore, evaluating the composition and properties for implementing a decision-making approach in material selection using up-to-date software is a topical problem in smart manufacturing. Therefore, the article aims to develop a comprehensive automated material selection approach. The proposed method is based on the comprehensive use of normalization and probability approaches and the linear regression procedure formulated in a matrix form. As a result of the study, analytical dependencies for automated material selection were developed. Based on the hypotheses about the impact of the phase composition on physical and mechanical properties, the proposed approach was proven qualitatively and quantitatively for carbon steels from AISI 1010 to AISI 1060. The achieved results allowed evaluating the phase composition and physical properties for an arbitrary material from a particular group by its mechanical properties. Overall, an automated material selection approach based on decision-making criteria is helpful for mechanical engineering, smart manufacturing, and industrial engineering purposes.

Keywords: mechanical properties; phase composition; process innovation; predictive maintenance; decision-making approach; industrial growth

MSC: 62J05; 90B50; 65F45; 15A24; 08A70



Citation: Pavlenko, I.; Piteľ, J.; Ivanov, V.; Berladir, K.; Mižáková, J.; Kolos, V.; Trojanowska, J. Using Regression Analysis for Automated Material Selection in Smart Manufacturing. *Mathematics* **2022**, *10*, 1888. <https://doi.org/10.3390/math10111888>

Academic Editors: Idelfonso B. R. Nogueira and Jozef Husar

Received: 6 May 2022

Accepted: 27 May 2022

Published: 31 May 2022

Publisher's Note: MDPI stays neutral with regard to jurisdictional claims in published maps and institutional affiliations.



Copyright: © 2022 by the authors. Licensee MDPI, Basel, Switzerland. This article is an open access article distributed under the terms and conditions of the Creative Commons Attribution (CC BY) license (<https://creativecommons.org/licenses/by/4.0/>).

1. Introduction

Traditionally, the choice of structural materials for designing machines is primarily determined based on calculations of strength, rigidity, stability, fatigue, and other static and dynamic loads [1]. However, in today's globalized market, the same structural materials may vary in their phase composition and physical and mechanical properties depending on the supplier country [2]. Therefore, the problem of determining the impact of the material's phase composition on its physical and mechanical properties (the direct problem), and vice versa (the inverse problem), is urgent in mechanical engineering. Its solution requires a comprehensive analysis of databases for various materials, compositions, and properties, including up-to-date computational means according to intelligent manufacturing tendencies.

The significance of the selected topic is highlighted by the following tendencies according to the Industry 4.0 strategy. Firstly, it is necessary to create automated data systems for materials transfer, compositions and properties, and subsequent aggregation as they become available and analyzed. Secondly, despite explicit documentation about the average values of the composition of the supplied material, critical parts are required to pass the input control of physical and mechanical properties. All these arrangements are especially relevant in turbomachinery, the aircraft industry, and so on. Moreover, the need to automate the corresponding designs and technical documentation is also a relevant problem.

In this regard, a number of scientific works in developing automated systems for material selection in smart manufacturing are analyzed below.

Bakhom and Brown [3] proposed an automated support system for choosing structural materials. As a result, the decision-making quality of sustainable selection was improved using a multi-attribute decision-making approach. Kolesnyk et al. [4] applied artificial neural networks to analyze a machining mode and surface accuracy. As a result, hole accuracy and drilling temperature were evaluated for drilling CFRP/Ti alloys.

Mafokwane and von Kallon [5] developed an approach to material selection for handling systems according to Industry 4.0 trends. As a result, a new design structure was validated based on the dependencies of the strength of materials in terms of deflections and stresses. Ivchenko et al. [6] developed a method for choosing cutting conditions. The proposed approach considered cutting conditions during precise turning of non-alloy carbon steel AISI 1045.

Kazemzadeh and Akis [7] described an evolutionary approach for the optimal automated selection of composite materials. The numerical simulation results proved the reliability of the proposed approach in designing multilayer composite tubes under internal pressure. Jghamou et al. [8] developed an automated decision-making approach for material and equipment selection based on the multiple-criteria decision analysis. The proposed methodology was implemented in the material selection for water pipes.

Akhmedzyanov et al. [9] implemented an automated material selection approach for the main parts of an aircraft engine. As a result, loads acting on the elements of the engine air-gas channel were evaluated. Srinivasan et al. [10] proposed a concept of an automated material selection for oil and gas production. The corresponding software system was developed to implement specific petroleum industry guidelines.

Veldenz et al. [11] applied the analytical hierarchy process to material selection for automated dry fiber placement. It was proven that this method is more preferred to predict the manufacturing quality for parts with complex geometry. Panchuk et al. [12] predicted the accuracy of the tapered thread profile for the case of lathe machining. Seo et al. [13] realized 3D building modeling based on an automated material selection and environmental assessment.

Treherm et al. [14] used artificial intelligence systems for material selection. As a result, the corresponding framework was designed for data-driven shape memory alloy discovery. Li et al. [15] applied machine learning with an improved genetic algorithm. As a result, material descriptor selection was realized for hardness prediction of high entropy alloys.

Lai et al. [16] studied the impact of material selection on the microstructure of deposited boron carbide coatings. Chatterjee and Chakraborty [17] applied a multi-attribute comparative analysis for the material selection of pistons from steel AISI 4140 and steel AISI 8660. Del Rosario [18] realized material selection based on the statistically rigorous reliability analysis. The proposed approach was complemented with statistical modeling to analyze composite laminate plates.

Kumar et al. [19] used a multi-criteria decision-making under uncertainties in material selection. Jahan et al. [20] applied a combined compromise solution method for material selection. As a result, a combined compromise solution method considered material selection for storage tank and wagon wall case studies.

Toledo et al. [21] applied multi-criteria means for alternative material selection in the automotive industry. Foong et al. [22] applied a structural optimization approach for

material selections. As a result, designs of multi-cantilevered vibration energy harvesters were improved. Also, Izonin et al. [23] proposed an approach for parameter evaluation by relatively small datasets based on general regression neural networks.

Altun et al. [24] described an approach to determining forces applied to elements of machines using artificial neural networks. Boyaci and Tuzemen [25] applied different multi-criteria decision-making approaches (i.e., a complex proportional assessment method) for material selection in the aerospace industry.

However, all the approaches mentioned above in material selection have some flows that should be eliminated. Firstly, it is impossible to explicitly control the influence of the phase composition of multicomponent materials on their physical and mechanical properties and vice versa. Secondly, it is still impossible to simultaneously solve direct and inverse problems based on a single approach. Thirdly, the methods used are unreasonably complicated in the applied algorithm and up-to-date computational means. These facts require powerful computational capabilities to implement complex algorithms and make their theoretical analysis practically impossible.

From the mathematical point of view, a multiply regression analysis can be used to solve the above-described problems. Generally, decision strategies using multiply regression analysis are described for example in [26]. One of the last publications regarding its application is using multiple regression analysis to predict directionally solidified TiAl mechanical properties [27].

The practical significance of the proposed methodology is in the ability to solve a direct and an inverse problem in automated material selection using a single approach for designing elements of machines in mechanical engineering, smart manufacturing, and industrial engineering.

Due to the above analysis, the main aim is to develop a comprehensive automated material selection approach. The following objectives have been formulated to achieve this aim. Firstly, an analytical approach for solving the direct and inverse problems of rational material selection based on the phase composition and physical and mechanical properties should be developed. Secondly, matrix dependencies for evaluating the physical and mechanical properties by the phase composition, and vice versa, should be proposed. Finally, the reliability of the proposed automated approach should be proven for particular case studies.

Overall, the main objectives correspond to the statement, recently concluded by Kangishwar et al. in 2022, that a better understanding of the significance of material selection approaches and their adaptability in various applications should be achieved [28].

During the study, the following hypotheses were formulated. Firstly, the relationships between phase compositions of a particular group of materials and related physical and mechanical properties are linear or weakly nonlinear (within a specific relative error). Secondly, if the dependence between the phase compositions and the physical and mechanical properties are known for this group, they will be reliable for an arbitrary unknown material within this group. All these hypotheses should be proven below by practical case studies.

2. Materials and Methods

2.1. The General Methodology

The proposed methodology is schematically represented in Figure 1. Its consequent stages include design calculation. The nominal mechanical properties are determined by analytical calculations of strength, stiffness, stability, etc. Traditionally, the stages mentioned above allow deciding on the material needed.

Nevertheless, for critical and highly loaded parts in high-tech industries, the mechanical properties of the selected materials must be confirmed by mechanical tests on the experimental samples. This is because even for widely used metals and alloys, their physical and mechanical properties can vary significantly depending on the supplier, the presence of impurities and the heat treatment modes, and other factors.

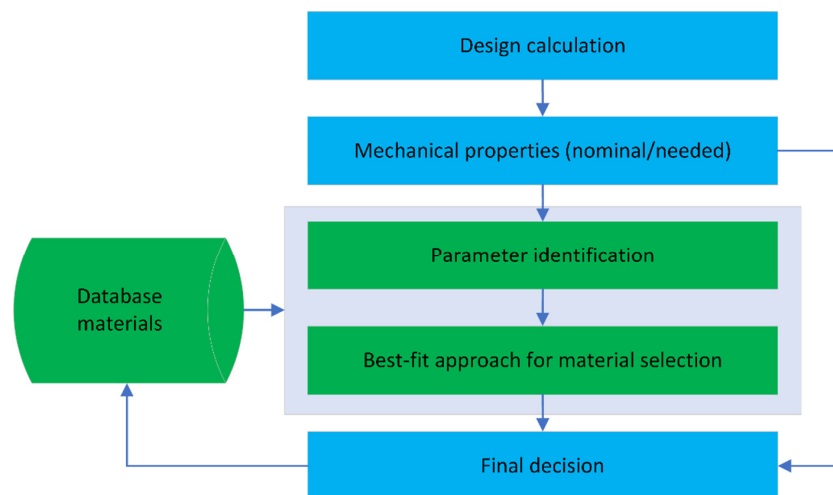


Figure 1. The scheme of the proposed methodology.

The following criteria are used to decide whether or not to implement green blocks in Figure 1. Firstly, high-quality structural material should meet a set of design requirements for structural strength. They should be selected as much as possible from the quantitative characteristics obtained in standard materials tests, e.g., conditional yield strength, ultimate tensile strength, relative elongation, relative narrowing, hardness, and fatigue limit. It is assumed that the deviation in the values of mechanical properties should be no more than 5% in the proposed methodology. It corresponds to the results of the work [29].

Secondly, the phase composition of any steel affects its structural strength. The most crucial element that determines the structure and properties of carbon steels is carbon. Carbon strongly affects steel properties, even with a slight change in its content. This is because the structure of carbon steel after slow cooling consists of two phases—ferrite and cementite. They have different properties depending on the ratio of these phases. Ferrite has low strength, low hardness, and good ductility, and cementite is a very hard and has a brittle phase. The ferrite's share with increasing carbon concentration in steel gradually decreases, and the share of cementite increases. Therefore, with an increasing amount of carbon, the hardness and strength of the steel itself increase (conditional yield strength, ultimate tensile strength), and the characteristics of ductility, elongation, and narrowing decrease.

The exact evaluation of carbon content in steel is the first and most crucial parameter identification, which is the basis of the proposed methodology for automatic material selection (the 1st green block). This identity parameter should be applied when the deviation in the chemical composition of carbon is 10% or more, which is consistent with [30].

In addition to the main components (iron and carbon), there are some impurities Mn, Si, S, P, and others in carbon steel. Mn and Si in tenths of a percent turn into steel in the process of its deoxidation; S and P in hundredths of a percent remain in steel due to the difficulty of their complete removal; Cr and Ni are converted into steel from a charge containing doped scrap metal, and are allowed in quantities of slightly more than 0.3% each. Relevant standards regulate permissible amounts of impurities in the steel. Impurities also affect the mechanical and technological properties of steel. For example, Mn and Si increase the hardness and strength, P gives the cold steel brittleness (brittleness at the normal and low temperatures), and S gives the steel's red brittleness (brittleness at the temperatures of hot pressure treatment). For high-quality carbon steels, higher composition requirements are set, e.g., lower sulfur (less than 0.04%), and phosphorus (less than 0.035%). Thus, the second identification parameter is the exact evaluation of the content of the above chemical elements (the 2nd green block) [31].

Therefore, based on the design requirements for the mechanical properties of the required material and considering the data of the 1st block, we apply the similarity criterion to search in the database material phase composition of the material with certain properties, which provides the best-fit approach (the 2nd green block).

For example, high-quality ferritic-pearlitic unalloyed medium-carbon structural steel AISI 1045 is one of the most used due to its price–quality combination. Its phase composition is 0.42–0.50% of C and less than 2.57% of impurities. However, this steel has different analogs related to its properties. Particularly, according to the standard ASTM A29/29M, steel 1045 has 0.43–0.50% of C; according to the standard DIN W-Nr, GB/T, and BS, steels DIN 1.1191/Ck45, 45, and 080M46 have 0.42–0.50% of C; according to the standard JIS, steel S45C has 0.42–0.48% of C. Also, the silicon content varies for different standards (e.g., $\leq 0.040\%$ —for the standards DIN W-Nr and BS, 0.17–0.37% for the standard GB/T, and 0.15–0.35% for the standard JIS). The manganese content also varies (e.g., 0.60–0.90% for the standards ASTM A29/29M and JIS, 0.50–0.80%—for the standards DIN W-Nr, GB/T, and BS, and 0.35–0.65% for the standard GOST 1050-88). Additionally, the total P and S content is less than 0.09% for the standard ASTM A29/29M, 0.07%—for DIN W-Nr, GB/T, and BS, and 0.06%—for JIS. Moreover, this steel has many equivalent replacements (e.g., USA—from 5135 to 5140RH, and from G51350 to H51400; European Union—from 37Cr4 to 41CrS4; Germany—1.7034 to 1.7045, and from 37Cr4 to 42Cr4; France—from 37Cr4 to 42C4TS; Spain—from 37Cr4 to 42Cr4, and from F.1201 to F.1211; UK—37Cr4, 41Cr4, and from 530A36 to 530M40; Japan—from SCr435 to SCr440H; China—from 35Cr to 45CrH, ML38CrA, and ML40Cr; Australia—5132H, and 5140).

As a result of such a different phase composition, physical and mechanical properties for analogs of steel AISI 1045 vary significantly. Particularly, for the different standards mentioned above, conditional yield strength $\sigma_{0.2}$ can vary from 310 to 495 MPa, ultimate tensile strength σ_B —from 550 to 725 MPa, and Brinell hardness HB —from 163 to 197–241 kgf/mm².

Therefore, the proposed approach includes a more comprehensive methodology (Figure 1). The decision-making approach implies determining the phase composition based on the data from the available databases. It ensures the best-fit approach for the rational choice of material considering different criteria (e.g., similarity criteria, mean square factor, etc.).

Finally, the regression analysis is implemented to clarify the physical and mechanical properties the final decision is made to confirm the type of material.

It has been applied for the carbon steel case study. For this purpose, steels from AISI 1010 to AISI 1060 have been considered. The chemical compositions of the carbon steels are presented in Table 1.

Table 1. The chemical composition of carbon steels, %. Adapted from [32,33].

Steel	C		Si		Mn		Cr	Other *
	x_1		x_2		x_3		x_4	x_5
	Min	Max	Min	Max	Min	Max		
AISI 1010	0.07	0.14					0.15	
AISI 1015	0.12	0.19			0.35	0.65		
AISI 1020	0.17	0.24						
AISI 1025	0.22	0.30						
AISI 1030	0.27	0.35						
AISI 1035	0.32	0.40	0.17	0.37			0.25	0.66
AISI 1040	0.37	0.45						
AISI 1045	0.42	0.50			0.50	0.80		
AISI 1050	0.47	0.55						
AISI 1055	0.52	0.60						
AISI 1060	0.57	0.65						
Maximum value of $X^{<j>}$ **	0.65		0.37		0.80		0.25	0.66

* Cu (0.25%) + Ni (0.25%) + As (0.08%) + S (0.04%) + P (0.04%). ** where j is order number of a phase component.

Averaged values of mechanical properties after the entire thermal treatment are summarized in Table 2.

Table 2. Mechanical properties. Adapted from [34,35].

Steel	Conditional Yield Strength $\sigma_{0.2}$, MPa	Ultimate Tensile Strength, σ_B , MPa	Relative Elongation-at-Break, δ_r , %	Relative Narrowing, ψ , %	Fatigue Limit, σ_{-1} , MPa	Brinell Hardness, HB, kgf/mm ²
	y_1	y_2	y_3	y_4	y_5	y_6
AISI 1010	260	420	32	69	187	143
AISI 1015	215	420	33	70	176	152
AISI 1020	245	470	29	72	206	161
AISI 1025	300	530	27	68	223	177
AISI 1030	415	585	23	65	255	163
AISI 1035	470	660	19	67	302	189
AISI 1040	485	730	17	62	323	208
AISI 1045	495	725	15	55	331	197
AISI 1050	490	710	15	55	421	200
AISI 1055	540	800	14	48	377	239
AISI 1060	590	920	12	50	373	229
Maximum value of $Y^{<l>}$ *	590	920	33	72	421	239

* where l —order number of physical and mechanical property.

This steel group was chosen since high-quality structural carbon steel of various brands is expected due to its low cost and high performance. It has a wide range of applications, so the proposed automated approach to selecting structural carbon steel based on decision criteria will be beneficial for mechanical engineering, intelligent production, and industrial engineering. Therefore, to reach this aim, it is appropriate to first solve the considered problem for non-alloy steel with minimum changes in chemical elements, which is typical for high-quality structural carbon steel.

These materials are widely used in machinery [36,37]. Particularly, steel AISI 1010 is used for designing bushings, screws, welding elements for tubular electric heaters and machine-building products, and cold-formed pipes for boilers and oil heaters. It is also used to produce corrosion-resistant multilayer sheets, elements of hydraulic systems of cars, combines, tractors, and refrigerators. Steel AISI 1015 is used for designing connecting nodes of metal structures, fittings, and bushings. Steel AISI 1020 is used to manufacture couplings, gears, and elements of worm pairs. Also, all kinds of fixtures for clamping parts and connecting elements between links of mechanisms (e.g., brackets, shafts) are made from it.

Axes, shafts, couplings, levers, forks, shafts, bolts, flanges, and fasteners are manufactured from steel AISI 2025. Steel AISI 2030 is widely used in aircraft, mechanical engineering, shipbuilding, and other civil and military industries. Elements of fittings at nuclear power plants, fasteners on pipelines, and boilers of thermal power plants are made from steel AISI 1035. Steel AISI 1040 is applied to manufacture high-strength parts, e.g., tubes, discs, shafts, and rotors in turbomachinery. Crankshafts, cylinders, spindles, and gears are made from steel AISI 1045.

Steel AISI 1050 is applied in designing parts operating under friction and high loads (e.g., gears, clutches, gearboxes, rods, axles, shafts, and springs). Steel AISI 1055 is widely used in the automotive industry to manufacture springs, railway transport, and other

machinery branches. Steel AISI 1060 is used to produce wheels, spindles, clutches, and other parts with high strength and wear resistance.

2.2. The Direct Problem

The direct problem is in the evaluation of the impact of material’s phase composition on its physical and mechanical properties based on the following matrix equation:

$$[X][A] = [Y], \tag{1}$$

where $[X]$ —matrix of the phase composition; $[Y]$ —matrix of the mechanical properties; $[A]$ —matrix of the weighted factors.

Matrix $[X]$ is rectangular with the dimension of $m \times n$, where m —the total number of the considered materials; n —the total number of the corresponding phase components. All elements $X_{i,j}$ are considered by the available databases of construction materials (i —order number of a material— $i = 1, 2, \dots, m$; order number of a phase component— $j = 1, 2, \dots, n$).

Matrix $[Y]$ is rectangular too, with the dimension of $m \times L$, where L —the total number of the valuable physical and mechanical properties. All elements $Y_{i,l}$ are also considered by the available databases of construction materials (l —order number of physical and mechanical property, $l = 1, 2, \dots, L$).

Therefore, matrix $[A]$ is rectangular with the dimension of $n \times L$. The elements $A_{i,j}$ should be evaluated based on the data from matrices of phase compositions $[X]$ and the corresponding physical and mechanical properties $[Y]$. However, this problem cannot be solved directly since all the values of $X_{i,j}$ are varied in a particular range between their minimum $X_{i,j}^{(min)}$ and maximum $X_{i,j}^{(max)}$ values.

Multiple groups of experiments applying random simulations are used to solve this problem. Therefore, matrix Equation (1) should be transformed to a generalized form:

$$[\bar{X}][A] = [\bar{Y}], \tag{2}$$

where matrix $[A]$ stays unchanged; $[\bar{X}]$ —extended matrix of the phase compositions. Its uniformly distributed values are normalized as follows:

$$(\bar{X}_{i,j})_k = \frac{X_{i,j}^{min} + rnd(X_{i,j}^{max} - X_{i,j}^{min})}{max(X^{(j)})}, \tag{3}$$

where k —order number of numerical experiment; $rnd(X)$ —a uniformly distributed random number between 0 and X .

Matrix $[\bar{Y}]$ is extended by the similar matrices $[Y]$ by k times with preliminary normalization. Its elements are as follows:

$$(\bar{Y}_{i,l})_k = \frac{Y_{i,l}}{max(Y^{(l)})}. \tag{4}$$

Overall, the first multiplier on the left of this equation is built by stacking all the randomly generated matrices $[X]_k$ within each k -th numerical experiment. The right part of this equation is also built by stacking all the randomly-generated matrices $[Y]_k$ within each k -th numerical experiment:

$$[\bar{X}] = \begin{bmatrix} [X]_1 \\ [X]_2 \\ \dots \\ [X]_N \end{bmatrix}; [\bar{Y}] = \begin{bmatrix} [Y]_1 \\ [Y]_2 \\ \dots \\ [Y]_N \end{bmatrix}, \tag{5}$$

where N —the total number of the numerical experiments ($k = 1, 2, \dots, N$).

Notably, all the elements $(\bar{X}_{i,j})_k$ and $(\bar{Y}_{i,l})_k$ are varied in a range from 0 to 1. The dimensions of matrices $[\bar{X}]$ and $[\bar{Y}]$ are $(k \cdot m) \times n$ and $(k \cdot m) \times L$, respectively.

Under the condition of $N \gg n$, Equation (2) can be solved concerning matrix $[A]$ using the following linear regression formula:

$$[A] = \left([\bar{X}]^T [\bar{X}] \right)^{-1} [\bar{X}]^T [\bar{Y}]. \tag{6}$$

Finally, the unknown matrix $[Y^{(e)}]$ of the mechanical properties can be evaluated from Equation (1):

$$[Y^{(e)}] = [X^{(av)}] [A], \tag{7}$$

where $[X^{(av)}]$ —averaged matrix of the phase composition, elements of which are determined as follows:

$$X_{i,j}^{(av)} = \frac{X_{i,j}^{min} + X_{i,j}^{max}}{2}. \tag{8}$$

Therefore, the direct problem is based on the comprehensive use of the probabilistic and regression approaches. In this case, the greater the total number N of numerical experiments, the more accurately the values of the estimated parameters are determined.

Programming of Formulas (3)–(8) for normalized parameters can be realized using a computer algebra system (Figure 2).

```

x(i,j,k) := x_min_i,j + md(x_max_i,j - x_min_i,j)

X := | for i ∈ 1..m
      |   for j ∈ 1..n
      |     X_i,j ← x(i,j,k)
      |   for k ∈ 2..N
      |     | for i ∈ 1..m
      |       |   for j ∈ 1..n
      |         |   ΔX_i,j ← x(i,j,k)
      |         |   Y ← stack(Y, ΔY)
      |         |   Y
      |       |
      |     | X ← stack(X, ΔX)
      |     |
      |     X

Y_r := | for i ∈ 1..m
       |   Y_i ← y_i,r
       |   for k ∈ 2..N
       |     | for i ∈ 1..m
       |       |   ΔY_i ← y_i,r
       |       |   Y ← stack(Y, ΔY)
       |       |
       |     | Y

A_r := (X^T · X)^-1 · X^T · Y_r

X_av := | for i ∈ 1..m
        |   for j ∈ 1..n
        |     X_av_i,j ← (x_min_i,j + x_max_i,j) / 2
        |   X_av

Y_e := X_av · A_r
    
```

Figure 2. Program realization using the computer algebra system MathCAD.

2.3. The Inverse Problem

The inverse problem is more valuable for practical purposes. This problem cannot be solved directly from the direct one since each element of matrix $[X]$ is changed in a

specific range. Therefore, the following modification is proposed. Let us consider the column-vector of L physical and mechanical properties for an arbitrary unknown material:

$$\{Y_0\} = \begin{Bmatrix} Y_1 \\ Y_2 \\ \dots \\ Y_L \end{Bmatrix}. \tag{9}$$

This material should be from the same material group of materials but with different physical and mechanical properties. According to this assumption, the dependence between these properties and unknown phase concentrations remains unchanged:

$$[A]^T \{X^{(e)}\} = \{Y_0\}, \tag{10}$$

where $\{X_0\}$ —column-vector of n unknown phase components:

$$\{X_0\} = \begin{Bmatrix} X_1 \\ X_2 \\ \dots \\ X_L \end{Bmatrix}. \tag{11}$$

If the total number L of unknown phase elements is not less than the total number n of measured physical and mechanical properties for the arbitrary material, Equation (10) can also be solved based on the following regression formula:

$$\{X^{(e)}\} = ([A][A]^T)^{-1} [A]\{Y_0\}. \tag{12}$$

2.4. Estimation Accuracy

The estimation accuracy can be estimated as follows. Particularly, the maximum relative error of the direct problem can be calculated:

$$\delta_{dir}^{max} = \max \left| \frac{Y_{i,l}^{(e)}}{Y_{i,l}} - 1 \right| \cdot 100\%. \tag{13}$$

The less the maximum relative error δ_{dir}^{max} , the higher the estimation accuracy for the direct problem.

The following normalized similarity criterion can prove the reliability of the proposed approach for solving the inverse problem in terms of different l -th phase components:

$$s_i^{(l)} = \frac{\left(\frac{X_{i,l}^{(av)}}{X_l^{(e)} - X_{i,l}^{(av)}} \right)^2}{\sum_{i=1}^m \left(\frac{X_{i,l}^{(av)}}{X_l^{(e)} - X_{i,l}^{(av)}} \right)^2}. \tag{14}$$

The higher the similarity criterion $s_i^{(l)}$, the higher the estimation accuracy for the i -th material by the l -th phase component.

Also, the overall normalized similarity criterion by all the phase composition elements can be:

$$\bar{s}_i = \frac{S_i - \min(S)}{\sum_{i=1}^m [S_i - \min(S)]}, \tag{15}$$

where S_i —the following unnormalized value:

$$S_i = \sum_{j=1}^n \left(\frac{X_{i,j}^{(av)}}{X_j^{(e)} - X_{i,j}^{(av)}} \right)^2 \tag{16}$$

The higher the overall similarity criterion \bar{s}_i , the higher the estimation accuracy for the i -th material by the entire phase composition.

Moreover, estimation accuracy can also be determined traditionally by the following root mean square:

$$RS_i = \sqrt{\frac{\sum_{j=1}^n (X_j^{(e)} - X_{i,j}^{(av)})^2}{n}} \tag{17}$$

The less the root mean square RS_i , the higher the estimation accuracy for the inverse problem.

Finally, after the rational choice of the i -th material by the condition of the minimum root mean square RS_i , the overall relative error is determined as follows:

$$\delta_e = \max \left| \frac{(Y_0)_l}{([Y]^T)_{l,i}} - 1 \right| \cdot 100\% \tag{18}$$

3. Results

3.1. Regression Dependencies

According to the data presented in Tables 1 and 2, the following parameters have been used: the total number of the considered materials— $m = 11$; the total number of the phases— $n = 5$; the total number of the evaluated mechanical properties— $L = 6$.

The normalized matrices of the minimum and maximum values for phase compositions from (3) are as follows:

$$[X^{min}] = \begin{bmatrix} 0.108 & 0.459 & 0.437 & 0.600 & 1.000 \\ 0.185 & 0.459 & 0.437 & 1.000 & 1.000 \\ 0.262 & 0.459 & 0.437 & 1.000 & 1.000 \\ 0.338 & 0.459 & 0.625 & 1.000 & 1.000 \\ 0.415 & 0.459 & 0.625 & 1.000 & 1.000 \\ 0.492 & 0.459 & 0.625 & 1.000 & 1.000 \\ 0.569 & 0.459 & 0.625 & 1.000 & 1.000 \\ 0.646 & 0.459 & 0.625 & 1.000 & 1.000 \\ 0.723 & 0.459 & 0.625 & 1.000 & 1.000 \\ 0.800 & 0.459 & 0.625 & 1.000 & 1.000 \\ 0.877 & 0.459 & 0.625 & 1.000 & 1.000 \end{bmatrix}; [X^{max}] = \begin{bmatrix} 0.215 & 1.000 & 0.813 & 0.600 & 1.000 \\ 0.292 & 1.000 & 0.813 & 1.000 & 1.000 \\ 0.369 & 1.000 & 0.813 & 1.000 & 1.000 \\ 0.462 & 1.000 & 1.000 & 1.000 & 1.000 \\ 0.538 & 1.000 & 1.000 & 1.000 & 1.000 \\ 0.615 & 1.000 & 1.000 & 1.000 & 1.000 \\ 0.692 & 1.000 & 1.000 & 1.000 & 1.000 \\ 0.769 & 1.000 & 1.000 & 1.000 & 1.000 \\ 0.846 & 1.000 & 1.000 & 1.000 & 1.000 \\ 0.923 & 1.000 & 1.000 & 1.000 & 1.000 \\ 1.000 & 1.000 & 1.000 & 1.000 & 1.000 \end{bmatrix} \tag{19}$$

The normalized matrices of the physical and mechanical properties from (4) are as follows:

$$[Y]_k = \begin{bmatrix} 0.441 & 0.457 & 0.970 & 0.958 & 0.444 & 0.598 \\ 0.346 & 0.457 & 1.000 & 0.972 & 0.418 & 0.636 \\ 0.415 & 0.511 & 0.879 & 1.000 & 0.489 & 0.674 \\ 0.508 & 0.576 & 0.818 & 0.944 & 0.530 & 0.741 \\ 0.703 & 0.636 & 0.697 & 0.903 & 0.606 & 0.682 \\ 0.797 & 0.717 & 0.576 & 0.931 & 0.717 & 0.791 \\ 0.822 & 0.793 & 0.515 & 0.861 & 0.767 & 0.870 \\ 0.839 & 0.788 & 0.455 & 0.764 & 0.768 & 0.828 \\ 0.831 & 0.772 & 0.455 & 0.764 & 1.000 & 0.837 \\ 0.915 & 0.870 & 0.424 & 0.667 & 0.895 & 1.000 \\ 1.000 & 1.000 & 0.364 & 0.694 & 0.886 & 0.958 \end{bmatrix} \tag{20}$$

After carrying out $N = 1 \times 10^4$ numerical experiments, the following randomly generated matrices (5) have been obtained:

$$\begin{aligned}
 [X] = & \begin{bmatrix} 0.108 & 0.564 & 0.657 & 0.600 & 1.000 \\ 0.203 & 0.844 & 0.551 & 1.000 & 1.000 \\ 0.368 & 0.524 & 0.441 & 1.000 & 1.000 \\ 0.359 & 0.703 & 0.646 & 1.000 & 1.000 \\ 0.523 & 0.976 & 0.827 & 1.000 & 1.000 \\ 0.588 & 0.998 & 0.854 & 1.000 & 1.000 \\ 0.615 & 0.826 & 0.628 & 1.000 & 1.000 \\ 0.749 & 0.722 & 0.904 & 1.000 & 1.000 \\ 0.797 & 0.857 & 0.840 & 1.000 & 1.000 \\ 0.864 & 0.866 & 0.688 & 1.000 & 1.000 \\ 0.895 & 0.536 & 0.885 & 1.000 & 1.000 \\ \dots & \dots & \dots & \dots & \dots \\ 0.929 & 0.998 & 0.972 & 1.000 & 1.000 \end{bmatrix} ; [Y] = \begin{bmatrix} 0.441 & 0.457 & 0.970 & 0.958 & 0.444 & 0.598 \\ 0.346 & 0.457 & 1.000 & 0.972 & 0.418 & 0.636 \\ 0.415 & 0.511 & 0.879 & 1.000 & 0.489 & 0.674 \\ 0.508 & 0.576 & 0.818 & 0.944 & 0.530 & 0.741 \\ 0.703 & 0.636 & 0.697 & 0.903 & 0.606 & 0.682 \\ 0.797 & 0.717 & 0.576 & 0.931 & 0.717 & 0.791 \\ 0.822 & 0.793 & 0.515 & 0.861 & 0.767 & 0.870 \\ 0.839 & 0.788 & 0.455 & 0.764 & 0.768 & 0.828 \\ 0.831 & 0.772 & 0.455 & 0.764 & 1.000 & 0.837 \\ 0.915 & 0.870 & 0.424 & 0.667 & 0.895 & 1.000 \\ 1.000 & 1.000 & 0.364 & 0.694 & 0.886 & 0.958 \\ \dots & \dots & \dots & \dots & \dots & \dots \\ 1.000 & 1.000 & 0.364 & 0.694 & 0.886 & 0.958 \end{bmatrix} . \quad (21)
 \end{aligned}$$

According to the linear regression Formula (6), the matrix of the weighted factors has been evaluated:

$$[A] = \begin{bmatrix} 0.823 & 0.668 & -0.850 & -0.478 & 0.751 & 0.470 \\ -0.006 & 0.000 & 0.004 & 0.003 & -0.011 & 0.000 \\ 0.147 & 0.040 & -0.113 & 0.027 & 0.040 & -0.002 \\ -0.238 & -0.090 & 0.072 & 0.229 & -0.154 & 0.008 \\ 0.362 & 0.376 & 1.133 & 0.880 & 0.397 & 0.518 \end{bmatrix} . \quad (22)$$

Therefore, after using the normalized averaged matrix (8) of the phase composition

$$[X^{(av)}] = \begin{bmatrix} 0.162 & 0.730 & 0.625 & 0.600 & 1.000 \\ 0.238 & 0.730 & 0.625 & 1.000 & 1.000 \\ 0.315 & 0.730 & 0.625 & 1.000 & 1.000 \\ 0.400 & 0.730 & 0.813 & 1.000 & 1.000 \\ 0.477 & 0.730 & 0.813 & 1.000 & 1.000 \\ 0.554 & 0.730 & 0.813 & 1.000 & 1.000 \\ 0.631 & 0.730 & 0.813 & 1.000 & 1.000 \\ 0.708 & 0.730 & 0.813 & 1.000 & 1.000 \\ 0.785 & 0.730 & 0.813 & 1.000 & 1.000 \\ 0.862 & 0.730 & 0.813 & 1.000 & 1.000 \\ 0.938 & 0.730 & 0.813 & 1.000 & 1.000 \end{bmatrix} , \quad (23)$$

The unknown normalized matrix of the mechanical properties can be evaluated from Equation (7):

$$[Y^{(e)}] = \begin{bmatrix} 0.439 & 0.457 & 0.970 & 0.958 & 0.444 & 0.598 \\ 0.407 & 0.457 & 1.000 & 0.972 & 0.418 & 0.636 \\ 0.415 & 0.511 & 0.879 & 1.000 & 0.489 & 0.674 \\ 0.508 & 0.576 & 0.818 & 0.944 & 0.530 & 0.741 \\ 0.703 & 0.636 & 0.697 & 0.903 & 0.606 & 0.682 \\ 0.797 & 0.717 & 0.576 & 0.931 & 0.717 & 0.791 \\ 0.822 & 0.793 & 0.515 & 0.861 & 0.767 & 0.870 \\ 0.839 & 0.788 & 0.455 & 0.764 & 0.768 & 0.828 \\ 0.831 & 0.772 & 0.455 & 0.764 & 1.000 & 0.837 \\ 0.915 & 0.870 & 0.424 & 0.667 & 0.895 & 1.000 \\ 1.000 & 1.000 & 0.364 & 0.694 & 0.886 & 0.958 \end{bmatrix} . \quad (24)$$

Each element $Y_{i,l}^{(e)}$ of the matrix (24) is highly close to the corresponding element $\bar{Y}_{i,l}$ of the matrix (24).

After using Formula (13), it can be concluded that 68% of the obtained data has the maximum relative error less than 6%, and only 12% of the obtained data exceed the maximum error of 10% (but only not more than 14%).

3.2. Rational Choice of the Material

For proving the reliability of the inverse problem, the arbitrary unknown material with the following mechanical properties is considered: conditional yield strength $\sigma_{0.2} = 517$ MPa, ultimate tensile strength $\sigma_B = 740$ MPa, relative elongation-at-break $\delta_r = 16\%$, relative arrowing $\psi = 56\%$, fatigue limit $\sigma_{-1} = 340$ MPa, and Brinell hardness $HB = 200$ kgf/mm².

All these data do not entirely fit all the rows in Table 2. Therefore, the direct problem of evaluating phase composition should be realized.

Firstly, the normalized physical and mechanical properties (9) can be calculated: $y_1 = 0.876$, $y_2 = 0.804$, $y_3 = 0.485$, $y_4 = 0.778$, $y_5 = 0.808$, and $y_6 = 0.837$.

Secondly, according to the linear regression formula (10), the normalized phase components are as follows: $x_1 = 0.687$, $x_2 = 0.756$, $x_3 = 0.829$, $x_4 = 0.989$, and $x_5 = 0.960$. Therefore, the estimated material has the following phase composition: 0.45% C, 0.28% Si, 0.66% Mn, 0.25% Cr, and 0.63% other components (Cu, Ni, As, S, and P).

The following criteria have been evaluated for deciding on which steel is most suitable for such a phase composited. Particularly, the normalized similarity criteria (14) for C and Mn have been calculated. Their maximum values of 0.90 and 0.11, respectively, are reached for $i = 8$. Additionally, the overall normalized similarity criterion (15) reached its maximum of 0.55 for $i = 8$. Moreover, the root means square (17) also reaches its minimum of 0.16 at $i = 8$. The above decision-making analysis results are represented graphically in Figure 3.

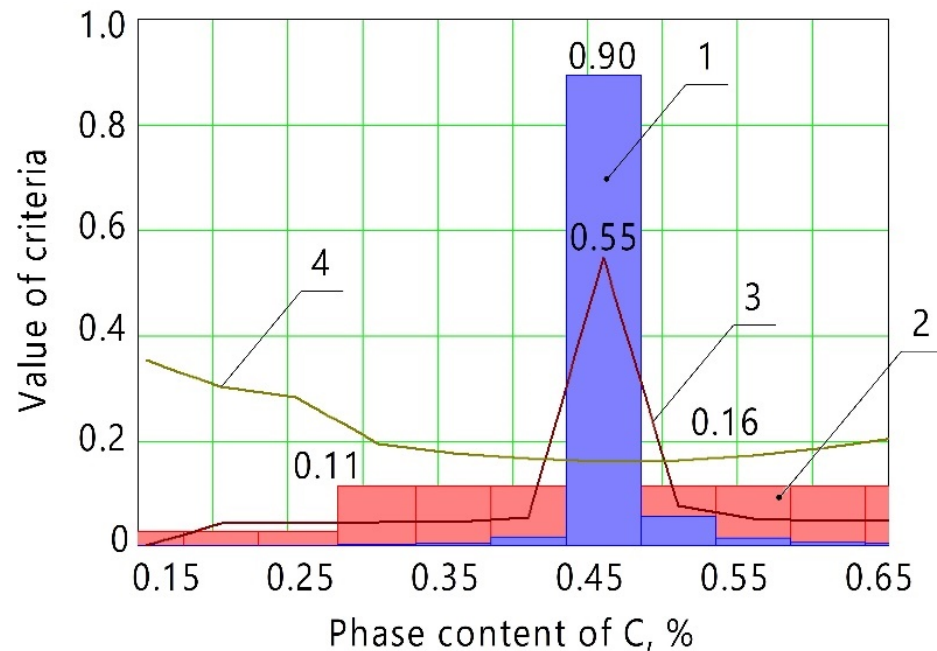


Figure 3. Graphical representation of the decision-making approach for material selection: 1—the normalized similarity criteria for C; 2—the normalized similarity criteria for Mn; 3—the overall normalized similarity criterion; 4—root mean square.

Therefore, the arbitrary unknown material is steel AISI 1045 (Table 1).

The test accuracy in terms of the phase composition evaluated by the proposed approach is presented in Table 3.

Table 3. The test accuracy for steel AISI 1045.

Phase Content	C	Si	Mn	Other *
Evaluated	0.45	0.28	0.66	0.63
Averaged by AISI [27,28]	0.46	0.27	0.65	0.66
Relative error, %	2.2	3.7	1.5	4.5

* Cu, Ni, As, S, and P.

Particularly, for steel AISI 1045, the maximum relative error does not exceed 5%.

4. Discussion

After a detailed analysis of this matrix, the following statements can be formulated. Values of $A_{1,1} = 0.823$, $A_{1,2} = 0.668$, and $A_{1,5} = 0.751$ indicate that an increase in carbon content significantly impacts an increase in conditional yield strength $\sigma_{0.2}$, ultimate tensile strength σ_B , and fatigue limit σ_{-1} . Also, $A_{1,3} = -0.850$ indicates that an increase in carbon content significantly impacts a decrease in relative elongation-at-break δ_r . These facts correspond to the results of the studies [38,39].

Insignificant values of $A_{2,l}$ indicate that an increase in silicon content does not pre-determine carbon steels' physical and mechanical properties. Additionally, a relatively small value of $A_{3,6}$ indicates that increased manganese content does not impact Brinell hardness HB of the carbon steels. These facts correspond to the results of the studies [40,41].

Moreover, values of $A_{5,3} = 1.133$, $A_{5,4} = 0.880$, and $A_{5,6} = 0.518$ indicate that an increase in the content of other additives (i.e., Cu, Ni, As, S, and P) can impact relative elongation-at-break δ_r , relative narrowing ψ , and Brinell hardness HB . This fact corresponds to the study results [42,43].

All these facts qualitatively prove the reliability of the developed approach.

The following data should be highlighted to compare the test accuracy between the proposed approach and other methods in material selection. Particularly, relative errors using neural networks [44] and weighted probabilistic neural networks [45] are up to 20%, the traditional machine learning algorithm [46]—12%, the probabilistic neural network-support vector machine algorithm [47]—8%, and convolutional neural networks [48]—5%. Therefore, the maximum relative error of up to 5% quantitatively proves the reliability of the proposed approach for material selection.

Therefore, the proposed methodology allows for designing an automated human-free database according to the Industry 4.0 strategy with the consequent accumulation of data as they are analyzed. Such an approach also allows realizing remote access to materials databases, which is especially important in automating up-to-date production design and technological preparation. Overall, all these approaches contribute to the digitalization of automated production, especially in manufacturing critical parts in machinery.

Further research directions will include implementing artificial neural networks to extend the proposed methodology for various materials (alloyed steels, composites, and so on) and implementing the corresponding database to software. Particularly, it is planned to use probabilistic neural networks and general regression neural networks.

5. Conclusions

A comprehensive automated material selection method has been developed according to the research results. It is based on a comprehensive application of the regression analysis and probability approach. Particularly, matrix dependencies for solving the direct and inverse problems of the rational material selection based on the phase composition and physical and mechanical properties have been proposed.

After the consequent normalization approach and linear regression formulas, analytical dependencies for evaluating the phase composition and physical and mechanical properties have been obtained.

The proposed automated approach has been analyzed qualitatively regarding the impact of the phase composition elements on physical and mechanical properties. The quantitative criteria for proving the reliability of the proposed methodology have also been calculated (i.e., the normalized and overall similarity criteria, root mean square, and relative errors). Particularly, for the carbon steel case study (from AISI 1010 to AISI 1060), the relative error does not exceed 5%.

Overall, the developed methodology evaluates an arbitrary material from its general group by measured physical and mechanical properties. It allows implementing an automated material selection using a single approach for designing elements of machines in mechanical engineering, smart manufacturing, and industrial engineering.

Author Contributions: Conceptualization, I.P. and K.B.; methodology, I.P. and J.P.; software, J.T. and V.I.; validation, K.B. and V.I.; formal analysis, J.P. and J.T.; investigation, I.P., J.P. and V.I.; resources, V.K. and J.T.; data curation, J.M. and K.B.; writing—original draft preparation, I.P. and K.B.; writing—review and editing, J.M. and V.I.; visualization, I.P. and V.K.; supervision, I.P. and J.T.; project administration, J.P. and V.I.; funding acquisition, J.P. and J.T. All authors have read and agreed to the published version of the manuscript.

Funding: This work was supported by the Slovak Research and Development Agency under the contract No. APVV-19-0590 and also by the projects VEGA 1/0700/20, 055TUKE-4/2020 granted by the Ministry of Education, Science, Research and Sport of the Slovak Republic.

Institutional Review Board Statement: Not applicable.

Informed Consent Statement: Not applicable.

Data Availability Statement: The data presented in this study are available on request from the corresponding author.

Acknowledgments: The scientific results have been partially obtained within the Joint Ukrainian-Slovak R&D Projects “Improvement of the Production Planning by Implementation of the Computer-Aided Fixture Design System” for the period of 2022–2023 granted by the Slovak Research and Development Agency (SK-UA-21-0060) and the Ministry of Education and Science of Ukraine. Also, the results have been partially obtained within the research project “Fulfillment of tasks of the perspective plan of development of a scientific direction “Technical sciences” Sumy State University” funded by the Ministry of Education and Science of Ukraine (State reg. no. 0121U112684). The authors appreciate the support of the Research and Educational Center for Industrial Engineering (Sumy State University) and the International Association for Technological Development and Innovations.

Conflicts of Interest: The authors declare no conflict of interest.

References

1. Harisha, M.S.; Ramesh, D.K.; Jayalakshmi, N. A study on design modification and validation by static and dynamic load analysis of SAE-1020 and 40C8 grade steel connecting rods of 4-stroke petrol engine. In *AIP Conference Proceedings*; AIP Publishing LLC: Melville, NY, USA, 2021; Volume 2316, p. 030027. [\[CrossRef\]](#)
2. Dulucheanu, C.; Severin, T.L.; Cerlinca, D.A.; Irimescu, L. Structures and mechanical properties of some dual-phase steels with low manganese content. *Metals* **2022**, *12*, 189. [\[CrossRef\]](#)
3. Bakhoun, E.S.; Brown, D.C. An automated decision support system for sustainable selection of structural materials. *Int. J. Sustain. Eng.* **2015**, *8*, 80–92. [\[CrossRef\]](#)
4. Kolesnyk, V.; Peterka, J.; Alekseev, O.; Neshta, A.; Xu, J.; Lysenko, B.; Sahul, M.; Martinovic, J.; Hrbal, J. Application of ANN for analysis of hole accuracy and drilling temperature when drilling CFRP/Ti alloy stacks. *Materials* **2022**, *15*, 1940. [\[CrossRef\]](#) [\[PubMed\]](#)
5. Mafokwane, S.Z.; von Kallon, D.V. Material Selection of a Tri-adjustable Automated Heavy-duty Handling System Designed on Industry 4.0 Principles. In *Proceedings of the 2nd South American Conference on Industrial Engineering and Operations Management, IEOM 2021, São Paulo, Brazil, 5–8 April 2021*; pp. 1606–1607.
6. Ivchenko, O.; Ivanov, V.; Trojanowska, J.; Zhyhylii, D.; Ciszak, O.; Zaloha, O.; Pavlenko, I.; Hladyshev, D. Method for an effective selection of tools and cutting conditions during precise turning of non alloy quality steel C45. *Materials* **2022**, *15*, 505. [\[CrossRef\]](#) [\[PubMed\]](#)
7. Kazemzadeh Azad, S.; Akış, T. Automated selection of optimal material for pressurized multi-layer composite tubes based on an evolutionary approach. *Neural Comput. Appl.* **2018**, *29*, 405–416. [\[CrossRef\]](#)

8. Jghamou, A.; Lahbabi, S.; Riane, F. Automated Decisional Process for Material and Equipment Selection: Application to the Selection of Material for Water Pipes. In Proceedings of the 11th Annual International Conference on Industrial Engineering and Operations Management, IEOM 2021, Singapore, 7–11 May 2021; pp. 5872–5883.
9. Akhmedzyanov, D.A.; Kishalov, A.E.; Markina, K.V. Automated Selection of the Material a Fan Blade PS-90A. In Proceedings of the 30th Congress of the International Council of the Aeronautical Sciences, ICAS 2016, Daejeon, Korea, 25–30 September 2016; p. 126186.
10. Srinivasan, S.; Kane, R.D.; Skogsberg, J.W. Automated material selection and equipment specification system for oil and gas production: Concept, development, implementation. *NACE-Int. Corros. Conf. Ser.* **2003**, *2003*, 135912.
11. Veldenz, L.; di Francesco, M.; Giddings, P.; Kim, B.C.; Potter, K. Material selection for automated dry fiber placement using the analytical hierarchy process. *Adv. Manuf. Polym. Compos. Sci.* **2018**, *4*, 83–96. [[CrossRef](#)]
12. Panchuk, V.; Onysko, O.; Kotwica, K.; Barz, C.; Borushchak, L. Prediction of the accuracy of the tapered thread profile. *J. Eng. Sci.* **2021**, *8*, B1–B6. [[CrossRef](#)]
13. Seo, S.; Tucker, S.; Newton, P. Automated material selection and environmental assessment in the context of 3D building modelling. *J. Green Build.* **2007**, *2*, 51–61. [[CrossRef](#)]
14. Trehern, W.; Ortiz-Ayala, R.; Atli, K.C.; Arroyave, R.; Karaman, I. Data-driven shape memory alloy discovery using artificial intelligence materials selection (AIMS) framework. *Acta Mater.* **2022**, *228*, 117751. [[CrossRef](#)]
15. Li, S.; Li, S.; Liu, D.; Zou, R.; Yang, Z. Hardness prediction of high entropy alloys with machine learning and material descriptors selection by improved genetic algorithm. *Comput. Mater. Sci.* **2022**, *205*, 111185. [[CrossRef](#)]
16. Lai, C.-C.; Boyd, R.; Svensson, P.-O.; Höglund, C.; Robinson, L.; Birch, J.; Hall-Wilton, R. Effect of substrate roughness and material selection on the microstructure of sputtering deposited boron carbide thin films. *Surf. Coat. Technol.* **2022**, *433*, 128160. [[CrossRef](#)]
17. Chatterjee, S.; Chakraborty, S. A multi-attributive ideal-real comparative analysis-based approach for piston material selection. *OPSEARCH* **2022**, *59*, 207–228. [[CrossRef](#)]
18. Del Rosario, Z. Precision materials indices: Materials selection with statistically rigorous reliability analysis. *AIAA J.* **2022**, *60*, 578–586. [[CrossRef](#)]
19. Kumar, D.; Marchi, M.; Alam, S.B.; Kavka, C.; Koutsawa, Y.; Rauchs, G.; Belouettar, S. Multi-criteria decision making under uncertainties in composite materials selection and design. *Compos. Struct.* **2022**, *279*, 114680. [[CrossRef](#)]
20. Jahan, F.; Soni, M.; Parveen, A.; Waseem, M. Application of combined compromise solution method for material selection. In Proceedings of the International Conference on Advancement in Materials, Manufacturing and Energy Engineering, ICAMME 2021, Online, 18–20 February 2021; pp. 379–387. [[CrossRef](#)]
21. Toledo, H.; Martínez-Gómez, J.; Nicolalde, J.F. Selection of rear axle tip alternative material of a car by multi-criteria means. *Int. J. Math. Oper. Res.* **2022**, *21*, 46–66. [[CrossRef](#)]
22. Foong, F.M.; Thein, C.K.; Yurchenko, D. Structural optimisation through material selections for multi-cantilevered vibration electromagnetic energy harvesters. *Mech. Syst. Signal Process.* **2022**, *162*, 108044. [[CrossRef](#)]
23. Izonin, I.; Tkachenko, R.; Gregus, M.; Zub, K.; Tkachenko, P. A GRNN-based approach towards prediction from small datasets in medical application. *Proc. Comput. Sci.* **2021**, *184*, 242–249. [[CrossRef](#)]
24. Altun, O.; Zhang, D.; Siqueira, R.; Wolniak, P.; Mozgova, I.; Lachmayer, R. Identification of dynamic loads on structural component with artificial neural networks. *Proc. Manuf.* **2020**, *52*, 181–186. [[CrossRef](#)]
25. Boyacı, A.Ç.; Tüzemen, M.Ç. Multi-criteria decision-making approaches for aircraft-material selection problem. *Int. J. Mater. Prod. Technol.* **2022**, *64*, 45–68. [[CrossRef](#)]
26. Takemura, K. *Escaping from Bad Decisions a Behavioral Decision-Theoretic Perspective*; Elsevier: Amsterdam, The Netherlands, 2021.
27. Kwak, S.; Kim, J.; Ding, H.; Xu, X.; Chen, R.; Guo, J.; Fu, H. Using multiple regression analysis to predict directionally solidified TiAl mechanical property. *J. Mater. Sci. Technol.* **2022**, *104*, 285–291. [[CrossRef](#)]
28. Kangishwar, S.; Radhika, N.; Sheik, A.A.; Chavali, A.; Hariharan, S. A comprehensive review on polymer matrix composites: Material selection, fabrication, and application. *Polym. Bull.* **2022**, in press. [[CrossRef](#)]
29. Sadowski, A.J.; Rotter, J.M.; Reinke, T.; Ummenhofer, T. Statistical analysis of the material properties of selected structural carbon steels. *Struct. Saf.* **2015**, *53*, 26–35. [[CrossRef](#)]
30. Tian, P.; Zhu, G.; Kang, Y. Effect of Carbon content on microstructure, properties and texture of ultra-thin hot rolled strip produced by endless roll technology. *Materials* **2021**, *14*, 6174. [[CrossRef](#)]
31. Salman, A.; Djavanroodi, F. Variability of chemical analysis of reinforcing bar produced in Saudi Arabia. In *IOP Conference Series: Materials Science and Engineering*; IOP Publishing: Bristol, UK, 2018; Volume 348, p. 012015. [[CrossRef](#)]
32. Gandy, D. *Carbon Steel Handbook*; EPRI: Palo Alto, CA, USA, 2007.
33. Hosford, W.F. *Iron and Steel*; Cambridge University Press: Cambridge, UK, 2012. [[CrossRef](#)]
34. Davis, J.R. *Mechanical Properties of Carbon and Alloy Steels*, 2nd ed.; ASM International: Russell Township, OH, USA, 1998. [[CrossRef](#)]
35. Phelps, C. *Carbon Steel: Microstructure, Mechanical Properties and Applications*; Nova Science Publishers: Hauppauge, NY, USA, 2019.
36. Islam, T.; Rashed, H.M.M.A. Classification and application of plain carbon steels. In *Reference Module in Materials Science and Materials Engineering*; Elsevier: Amsterdam, The Netherlands, 2019.

37. Angelo, P.C.; Ravisankar, B. *Introduction to Steels: Processing, Properties, and Applications*, 1st ed.; Taylor & Francis Group: Abingdon, UK, 2019.
38. Lv, Z.; Qian, L.; Liu, S.; Zhan, L.; Qin, S. Preparation and mechanical behavior of ultra-high strength low-carbon steel. *Materials* **2020**, *13*, 459. [[CrossRef](#)]
39. Johnson, O.T.; Ogunmuyiwa, E.N.; Ude, A.U.; Gwangwavac, N.; Addo-Tenkorang, R. Mechanical properties of heat-treated medium carbon steel in renewable and biodegradable oil. *Proc. Manuf.* **2019**, *35*, 229–235. [[CrossRef](#)]
40. Kim, B.; Sietsma, J.; Santofimia, M.J. The role of silicon in carbon partitioning processes in martensite/austenite microstructures. *Mater. Des.* **2017**, *127*, 336–345. [[CrossRef](#)]
41. Salvetr, P.; Nový, Z.; Gokhman, A.; Kotous, J.; Zmeko, J.; Motyčka, P.; Dlouhý, J. Influence of Si and Cu content on tempering and properties of 54SiCr6 steel. *Manuf. Technol.* **2020**, *20*, 516–520. [[CrossRef](#)]
42. Kučerová, L.; Jirková, H.; Volkmanová, J.; Vrtáček, J. Effect of aluminium and manganese contents on the microstructure development of forged and annealed TRIP steel. *Manuf. Technol.* **2018**, *18*, 605–610. [[CrossRef](#)]
43. Salvetr, P.; Gokhman, A.; Nový, Z.; Motyčka, P.; Kotous, J. Effect of 1.5 wt% Copper addition and various contents of silicon on mechanical properties of 1.7102 medium carbon steel. *Materials* **2021**, *14*, 5244. [[CrossRef](#)]
44. Duriagina, Z.A.; Tkachenko, R.O.; Trostianchyn, A.M.; Lemishka, I.A.; Kovalchuk, A.M.; Kulyk, V.V.; Kovbasyuk, T.M. Determination of the best microstructure and titanium alloy powders properties using neural network. *J. Achiev. Mater. Manuf. Eng.* **2018**, *87*, 23–30. [[CrossRef](#)]
45. Kusy, M.; Kowalski, P. Weighted probabilistic neural network. *Inf. Sci.* **2018**, *430*, 65–76. [[CrossRef](#)]
46. Kumar, A.; Sharma, R.; Gupta, A.K. Experimental investigation of WEDM process through integrated desirability and machine learning technique on implant material. *J. Mech. Behav. Mater.* **2021**, *30*, 38–48. [[CrossRef](#)]
47. Izonin, I.; Tkachenko, R.; Gregus, M.; Duriagina, Z.; Shakhovska, N. PNN-SVM approach of Ti-based powder's properties evaluation for biomedical implants production. *CMC-Comput. Mater. Contin.* **2022**, *71*, 5933–5947. [[CrossRef](#)]
48. Xie, X.; Bennett, J.; Saha, S.; Lu, Y.; Cao, J.; Liu, W.K.; Gan, Z. Mechanistic data-driven prediction of as-built mechanical properties in metal additive manufacturing. *Comput. Mater.* **2021**, *7*, 86. [[CrossRef](#)]